

FROM PHYSICAL TO LOGICAL: GRAPH-STATE-BASED CONNECTIVITY IN QUANTUM NETWORKS

MATEO M. BLANCO, MANUEL FERNÁNDEZ-VEIGA, ANA FERNÁNDEZ-VILAS, REBECA P. DÍAZ-REDONDO

ABSTRACT. Entanglement is a key resource in quantum communication, but bipartite schemes are often insufficient for advanced protocols like quantum secret sharing or distributed computing. Graph states offer a flexible way to represent and manage multipartite entanglement in quantum networks, enabling logical connectivity through local operations and classical communication (LOCC). In this work, we extend existing approaches based on bi-star configurations to more complex multi-star topologies. We analyze the maximum connectivity that can be achieved in networks of m switches, each connected to n clients, including asymmetric cases where the number of clients varies per switch. We also propose methods to enable logical communication between distant nodes. Our results support the development of scalable quantum networks with rich connectivity beyond traditional bipartite structures.

KEYWORDS: Graph states, entanglement, virtual graphs, quantum networks.

1. INTRODUCTION

Entanglement and, notably, the distribution of entangled pairs along with entanglement swapping and purification forms the foundations in the development of the quantum internet and quantum communications, with its unique properties enabling secure and efficient information transfer across distant locations [1, 2, 3, 4]. However, bipartite entanglement becomes insufficient when exploring complex quantum protocols beyond simple QKD, including quantum secret sharing, quantum error correction, and multipartite QKD. More complex entangled states, such as GHZ states, are challenging to generate using basic entanglement processes such as entanglement swapping. To address these shortcomings, Graph States [5] offer a structured framework for generating multipartite entanglement in quantum networks by associating entanglement with graph edges and enabling transformations via LOCC operations [6].

This approach allows for flexible, scalable entanglement distribution while preserving the network’s physical structure. Theoretical [7, 8, 9] and experimental [10, 11] studies confirm their benefits in optimizing network resources. From the quantum networking perspective, graph states have been proposed as the core architecture for all-photonic quantum repeaters within a network [12]. Applying LOCC operations and measurements to graph states alters the topology of the logical network and allows one to connect initially disconnected nodes. As classical network reachability supports the ability of a node to successfully communicate with another node in the network, quantum reachability should establish and maintain entanglement

This work was supported under the grants TED-2021-130369B-C31 funded by MICIU/AEI/10.13039/501100011033 by the “European Union NextGenerationEU/PRTR”; PID2023-148716OB-C31 funded by MICIU/AEI/10.13039/501100011033; grant ED431B 2024/41 (GPC) by the Galician Regional Government; and the regional agreement for laboratories and demonstration centers in cybersecurity within the RETECH program.

between two nodes anywhere in the network, enabling communication and, as an extension, distributed quantum protocols.

In this paper, we follow the approach in [13] to obtain artificial topologies from the physical ones by manipulating bi-colorable graph states through local operations. Reference [13] provides protocols to achieve various connectivity schemes from a bi-star configuration: peer-to-peer—all leaves of one star graph are connected to a leaf in the other; role delegation—one of the leaves acts as the center of the star topology; and extranet—all leaves are interconnected, forming a $|K_{n_1, n_2}\rangle$ graph state. In parallel, Quantum Local Area Networks (QLANs) are introduced in [14], as a star graph with a central switch and multiple leaf nodes representing clients. When central nodes in the stars are connected by quantum channels, a bi-star configuration emerges, i.e., two star graphs joined through entanglement of their respective centers. Finally, [15] establishes a strong upper bound on the maximum neighbor connectivity in a linear cluster state, $\alpha \leq \lfloor \frac{n+3}{2} \rfloor$, where n is the number of elements in the cluster.

We seek the generalization of the approaches above to extend their applicability to more complex network architectures. Specifically, for a linear graph consisting of m stars, each with n nodes (leaves), the maximum entangled states that can be generated have not been fully characterized. In this work, we partially characterize these maximal entangled states, leveraging multipartite entanglement and its implementation in graph states to overcome the limitations of traditional bipartite entanglement-based communication. Precisely, our contributions are as follows: (1) characterizing the maximum achievable connectivity for a general multi-star network with m switches, each connected to n nodes (leaves); (2) analyzing scenarios where each switch has a different number of nodes; and (3) developing a method to enable communication between two or more nodes in the network.

2. THEORETICAL PRELIMINARIES

Since the formalism of graph states builds upon the basic concepts of graph theory, we briefly review in this Section the necessary definitions and properties.

A graph $G = (V, E)$ consists of a set of vertices V connected pairwise by edges E . Its extension to graph states in quantum mechanics is both straightforward and profound: the vertices of the graph correspond to qubits, each initialized in the state $|+\rangle = \frac{1}{\sqrt{2}}(|0\rangle + |1\rangle)$, while the edges represent controlled- Z (CZ) gates that entangle the connected qubits. Under these assumptions, a graph state is formally defined as

$$|G\rangle = \prod_{e \in E} CZ |+\rangle^{\otimes |V|}.$$

where CZ, in the basis $\{|00\rangle, |01\rangle, |10\rangle, |11\rangle\}$, applies a Pauli- Z to the second input qubit only when the first qubit is $|1\rangle$. A simple example illustrates the entanglement structure: a graph consisting only of two connected vertices forms a Bell state, i.e., $|G\rangle = CZ(|+\rangle, |+\rangle) = \frac{1}{\sqrt{2}}(|\phi^-\rangle + |\psi^+\rangle)$, where the usual Bell states have been denoted as $|\phi^\pm\rangle = \frac{1}{\sqrt{2}}(|00\rangle \pm |11\rangle)$, $|\psi^\pm\rangle = \frac{1}{\sqrt{2}}(|01\rangle \pm |10\rangle)$. Since graph states are built from their classical graph counterparts, their fundamental properties and basic definitions remain similar. First, the neighborhood of a vertex $i \in V$ in the graph $G = (V, E)$ is the set of nodes directly connected to i , $N_i = \{j \in V : (i, j) \in E\}$. A path is a sequence of edges that connects a sequence of distinct vertices. If the initial and final vertices coincide, the path forms a cycle. A tree is a connected acyclic graph—a unique path exists between any pair of nodes—and the nodes of degree 1 in a tree (nodes with only one neighbor) are called the leaves of the tree. A caterpillar is a tree such

that the removal of leaves results in a path. A star is a tree where all the nodes but one are leaves, equivalently, if deletion of all the leaves results in a single node without edges.

The logical structure of a graph state may be modified by means of the application of Pauli measurements. Each of these will induce local changes in the measured qubit and its vicinity, altering the entanglement relationships among the existing qubits and thus changing the structure of the graph state and correspondingly the virtual topology of the network of states. More specifically, these effects will be a combination of the following elementary transformations on a graph. Given a subset of nodes $A \subset V$, the induced subgraph of A will be denoted as $G[A] = (A, E_A)$, and is the subgraph with edges $E_A = \{(i, j) \in E : i \in A \wedge j \in A\}$ obtained after deleting from G all the vertices not in A and their edges.

- (i) **Graph complementation.** Let $G = (V, E)$ be a graph. The complement of G , denoted as $\tau(G)$ is the graph (V, \bar{E}) , where

$$\bar{E} = V^2 \setminus E = \{(i, j) \in V^2 : (i, j) \notin E\}.$$

Clearly, $G \cup \tau(G)$ is the *complete graph* on $|V|$ vertices, i.e., the graph wherein any pair of vertices is connected by an edge. The complete graph with n nodes will be denoted hereafter as K_n .

- (ii) **Local complementation.** Of particular interest for graph states is the local complementation at a vertex i . This operation consists of taking the complement of the neighborhood of i . Accordingly, the local complementation at i is

$$\tau_i(G) = (V, (E \cup N_i^2) \setminus E_{N_i}),$$

where E_{N_i} is the set of edges in the neighborhood N_i of i . The resulting graph $\tau_i(G)$ has the same vertex set V as G , but the edges within N_i are deleted, and all the edges missing between pairs of nodes in N_i are appended. This local operation corresponds to a sequence of local Clifford operations, as described in [6].

- (iii) **Vertex deletion**, where a graph G is transformed into G_{-i} by removing a vertex i and all its associated edges:

$$G_{-i} = (V \setminus \{i\}, E \setminus (\{i\} \times N_i)).$$

Though the operation of local complementation may initially appear abstract, it actually aligns with a fundamental concept in quantum mechanics: **Local Unitary equivalence (LU)**. Two n -qubit graph states, $|G\rangle$ and $|G'\rangle$, are said to be LU equivalent if there exists a set of local unitaries $\{U_i\}_{i \in I}$ such that

$$|G'\rangle = \bigotimes_{i \in I} U_i |G\rangle,$$

so that it is possible to transform $|G\rangle$ into $|G'\rangle$ by a sequence of local quantum operations. For the special case of local complementation of a vertex a and its neighborhood N_a , the corresponding unitary transformation is given by

$$(1) \quad U_a^T = e^{-i\frac{\pi}{4}\sigma_{X_a}} \bigotimes_{b \in N_a} e^{i\frac{\pi}{4}\sigma_{Z_b}},$$

where σ_{X_a} is the application of a Pauli X operator to vertex a . Indeed, local complementation is an LU equivalence, with the corresponding unitary transformation given by Eq. 1.

Example 1 (Local complementation). *As shown in the Fig. 1, when vertex d is selected, the edges connecting its neighbors that were previously present are removed, while new edges are formed between those neighbors that were not previously connected.*

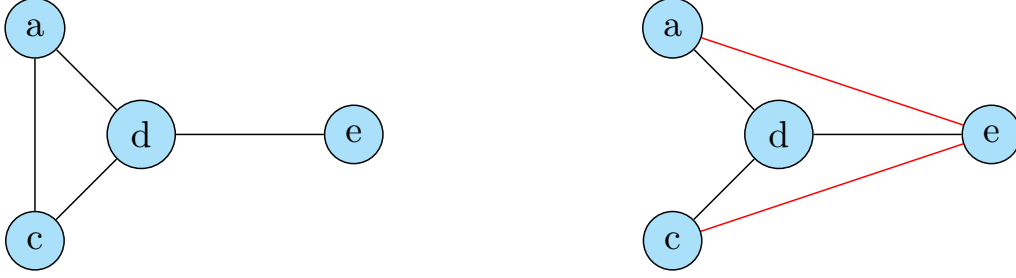


FIGURE 1. Example of local complementation at vertex d . Added edges are colored in red.

On the other hand, an useful example of local complementation and LU equivalence is the transformation between a complete graph K_n of n vertices $|K_n\rangle$ and a star graph with $n - 1$ leaf nodes and a central node, $|S_{n-1}\rangle$. This is achieved by performing local complementation of K_n at any node, so that this node becomes the center of S_{n-1} .

The effect of Pauli measurement on a graph state can be summarized in the following key result [5]

Theorem 1 (Pauli Measurements on Vertex i). *Let $G = (V, E)$ be a graph with $|V| = n$ nodes. The graph $\tilde{G} = (\tilde{V}, \tilde{E})$, with $|\tilde{V}| = n - 1$, obtained after a Pauli measurement on qubit i is as follows.*

- (i) *Pauli Z. $\sigma_{Z_i}(G) := \tilde{G} = G_{-i}$ the deletion of vertex i .*
- (ii) *Pauli Y. $\sigma_{Y_i}(G) := \tilde{G} = (\tau_i(G))_{-i}$ corresponds to a local complementation at i , followed by the deletion of i .*
- (iii) *Pauli X. $\sigma_{X_i}(G) := \tilde{G} = \tau_{k_0}(\tau_i(\tau_{k_0}(G))_{-i})$ for an arbitrary node $k_0 \in N_i$. The new graph is the local complementation of G at the neighbor k_0 , followed by a local complementation at i , the deletion of i , and a final local complementation at k_0 .*

3. PROBLEM STATEMENT

By using Theorem 1, it should be possible to transform an initial graph state $|G\rangle$ into another one $|G'\rangle$ particularly suited to some specific quantum protocol, or to manipulate an initial multipartite quantum state for some communication task (quantum or entanglement-assisted but classical). The sequence of measurements that lead to such a desired target state will be termed a *graph protocol*. However, since $CZ^2 = I$, we need that the multipartite states that our graph protocol manipulates must be bi-colorable, where a graph is said to be bi-colorable when its vertex set V can be partitioned into two subsets $\{P_1, P_2\}$ such that no two vertices within the same subset are adjacent. Many interesting quantum network models naturally emerge as bi-colored graphs, allowing for the derivation of practical results. Under this assumption, suppose $|G\rangle$ is a graph state whose underlying graph G is bi-colorable. We seek to characterize what bi-colorable graph states $|G'\rangle$ are achievable through a graph protocol \mathcal{T} composed of a sequence of Pauli measurements, $|G\rangle \xrightarrow{\mathcal{T}} |G'\rangle$. The graph protocol must avoid those sequences that may disrupt bi-colorability.

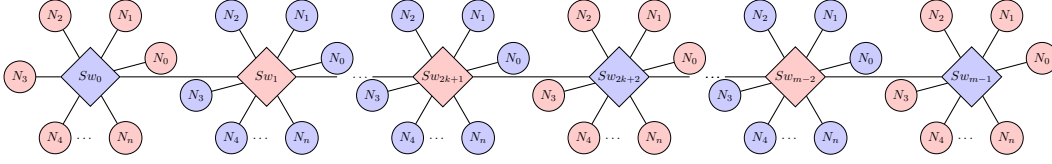


FIGURE 2. Multi-star configuration as an example of a linear network.

Bi-colorable graphs are of significant importance in quantum graph states theory because they enable the implementation of error correction and purification protocols [16, 17]. This idea has been further explored in the context of so-called quantum local area network (QLAN) architectures [18]. Despite the constraints imposed by the bi-colorable condition, the advantages provided by this class of graphs outweigh these restrictions. One such canonical graph is the binary star graph: two star graphs joined at their central nodes. It will be denoted as S_{n_1, n_2} , where Sw_1 represents the center of the first star and Sw_2 is the center of the second star. The remaining vertices are partitioned into sets N_i^1 and N_j^2 , where $i \in \{1, \dots, n_1\}$ and $j \in \{1, \dots, n_2\}$. This binary star graph can be constructed from two independent star graphs via a remote CZ operation applied to their central nodes. The extension of such entanglement generation between their centers converts an arbitrary number of isolated stars connected into a connected multi-star configuration, see Fig. 2.

4. ACHIEVABLE MULTIPARTY CONNECTIVITY THROUGH GRAPH-STATE MANIPULATIONS

Consider a network in the form of a multi-star topology, as shown in Fig. 2. The multi-star is a sequence of star subgraphs where the centers of the stars are connected in a line graph. We will refer to the centers Sw_i node in a star i as a *switch* and to its peripheral leaf nodes N_i as its *clients*, and assume that the stars have a variable number of leaves. Our goal is to characterize the achievable network connectivity on these nodes, where connectivity means the establishment of multipartite entanglement among an arbitrary subset $S \subseteq \cup_{i \in I} N_i$ of clients, if this is feasible. Specifically, we assume that each star subgraph represents the existence of a shared GHZ state $|\text{GHZ}_{n+1}\rangle := \frac{1}{\sqrt{2}}(|0\rangle^{\otimes(n+1)} + |1\rangle^{\otimes(n+1)})$ among the switch and its n leaves, and we seek to determine the largest GHZ state that can be realized in a general network consisting of m of these switches using the minimum number of measurements on the original graph states. In summary, the multi-star representation is particularly useful because it aligns naturally with a physical quantum switch configuration with the end-nodes as the clients; and the extended (largest) entangled state can then be used for implementing a multi-partite quantum protocol (see Subsection 6.2)

As a first step, we first establish a method to achieve the maximum neighbor configuration starting from a multi-star topology.

4.1. Maximum neighbor configuration. Recent works [15] have explored *linear* graph states (or cluster states) and their transformation into maximal $|\text{GHZ}\rangle$ configurations. In fact, [15] establishes a strict upper bound for an arbitrarily long linear cluster state, given by $\alpha_0 \leq \lfloor \frac{m+3}{2} \rfloor$, where m represents the number of linear nodes in the cluster, and the equality holds for an odd number of switches. While the proofs of these theorems are compelling and neat, the addition of leaf nodes to each switch, as in our case, further complicates the protocol and requires a refinement in the arguments. An important remark is that, in both cases, the

Algorithm 1 Maximally Connected Graph from linear graph state $|G\rangle$ with odd number of m switches and n leaves per S_w .

```

1: function ACHIEVEMAXCONNECTEDGRAPH( $|G\rangle, m, n$ )
2:    $P_0 \leftarrow \{\text{nodes color 0}\} ; P_1 \leftarrow \{\text{nodes color 1}\}$  ▷ bi-colored set of nodes
3:    $E \leftarrow E_S \cup E_{n_i}$  ▷ edges between  $S_{w_i} S_{w_{i+1}}$  and edges corresponding to leaves  $K_j^i$  in a
    $S_{w_i}$ 
4:    $G = (P_0, P_1, E)$  ▷ Resulting bi-colored graph  $G$ 
5:   for  $odd \in \{m \bmod 2\}$  do ▷ Leave  $S_{w_0}$  and  $S_{w_{m-1}}$  untouched and select Odd switches
6:      $\sigma_Z(\{K_{odd}^k\})$  ▷  $n$  measurements  $Z$  on leaf nodes of every switch  $S_{w_{odd}}$ 
7:      $\sigma_X(\{S_{w_{odd}}\})$  ▷ A measurement  $X$  on every switch  $S_{w_{odd}}$  with  $k_0$  as its right
   neighbouring switch
8:   return  $G' = (P'_0, P'_1, E')$  ▷ Maximally Connected Graph with  $(n+1)\frac{(m+1)}{2}$  vertices.

```

post-measurement state is locally Clifford equivalent to the GHZ state via local complementation. We present the modified measurement protocol as [Algorithm 1](#). For our problem, we have the following simple result.

Proposition 1. *Given a multi-star graph G of m switches and n nodes each, m is an odd number of and $n \in \mathbb{N}$, the complete graph K_α is achievable with [Algorithm 1](#) for $\alpha = (n+1)\frac{m+1}{2}$.*

Proof. The result can be derived by following directly the steps in the algorithm. We start with all the $m(n+1)$ nodes and then subtract the number of measurements performed. First, we measure the leaf nodes of every other switch, totaling $n\frac{m-1}{2}$. After that, we apply σ_X gates on the remaining switches, transforming the network into a star graph. This yields a total of

$$m(n+1) - n\frac{m-1}{2} - \frac{m-1}{2} = (n+1)\left(m - \frac{m-1}{2}\right).$$

Thus, we arrive at the expression $\alpha = (n+1)\frac{m+1}{2}$ clients completely connected. The cost of this transformation, the number of necessary measurements, is $(n+1)\frac{m-1}{2}$. \square

Clearly, we observe that the result for α_0 in cluster graphs, formally proven in [15] is not recovered when taking the limit $n \rightarrow 0$. This discrepancy arises from the topological differences between the two networks: while a linear cluster resembles a one-dimensional structure, a multi-star graph does not.

Next, consider an even-numbered multi-star graph, and let us follow a similar procedure to [Algorithm 1](#). We begin by leaving the first and last nodes untouched and perform measurements on the leaf nodes of every one of the alternating $(m-2)/2$ switches. This leads to a discrepancy when we reach the final measurement step: both $S_{w_{m-2}}$ and $S_{w_{m-1}}$ retain their leaf nodes: $S_{w_{m-1}}$ due to the initial hypothesis and $S_{w_{m-2}}$ because of the alternating measurement pattern. So, at this stage, we must additionally remove the leaf nodes of $S_{w_{m-2}}$, which results in two consecutive leafless switches by graph complementation. Consequently, the complete graph connectivity is reduced, since we must perform a σ_Y measurement on $S_{w_{m-2}}$ to proceed with the standard algorithm. In summary, when dealing with networks having an even number of switches, we must first transform it into an odd-numbered network of switches in order to be able to apply the proposed algorithm. Since we cannot assume that introducing additional switches with leaf nodes is allowed, we conclude that the only possibility is to remove at least one switch, thereby strictly reducing the network size by one star.

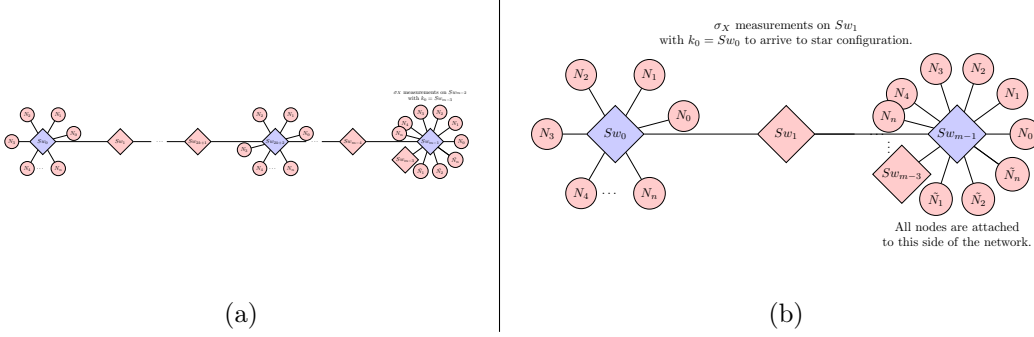


FIGURE 3. Steps of [Algorithm 1](#) for the case of an odd number of switches over a full linear network including the switches Sw_i and their clients N_j . Clients are eliminated through σ_Z measurements in every other node. (a) Starting from the second-to-last node, σ_X measurements are performed on the lone switches, with k_0 being the right neighbor. (b) In the final step, all nodes accumulate at the last switch. A final σ_X measurement in Sw_1 results in the formation of a star configuration that is LC equivalent to a complete graph.

4.2. Different number of leaf nodes in each switch. We now aim to calculate the maximum allowed connectivity for a more realistic linear network where each switch has a different number of leaf nodes. Suppose that the network consists of m switches, with each switch connected to n_0, n_1, \dots, n_{m-1} leaf nodes, respectively. Let us define $T = \{n_0, \dots, n_{m-1}\}$ as the total set of leaf nodes. The total number of nodes in the network is given by $N_T = m + \sum_{i=0}^{m-1} n_i$. To determine the maximum number of neighbors remaining, we calculate the total number of nodes and subtract the number of measurements performed. since each measurement removes a node from the network. We consider the case where m is odd and proceed again according to the steps outlined in [Algorithm 1](#). First, select $\frac{m-1}{2}$ switches to perform σ_Z operations onto. As discussed previously, these switches are chosen so as to remove all leaf nodes from every other switch. Thus, the set of selected nodes is $I = \{n_1, n_3, \dots, n_{m-2}\}$, and the total number of measurements made during this step is $M_1 = \sum_{i \in I} n_i$. Next, we perform $\frac{m-1}{2}$ σ_X operations. This step also contributes a total of $M_2 = \frac{m-1}{2}$, and results in the star configuration $|S_{\tilde{n}_1}\rangle$ with $\tilde{n}_1 = \frac{m-1}{2} + \sum_{i \in T \setminus I} n_i$. Therefore, the total number of measurements implemented on the network is given by $M_T = M_1 + M_2 = \frac{m-1}{2} + \sum_{i \in I} n_i$, and subtracting this from the total number of nodes, we obtain the remaining neighbors as $N_T - M_T = \frac{m-1}{2} + \sum_{i \in T \setminus I} n_i$, where $T \setminus I = \{n_{2i}\}_{i=0}^{\frac{m-1}{2}}$. Thus, the new maximum neighbor connectivity for the original α is given by $\tilde{\alpha} = \frac{m+1}{2} + \sum_{i \in T \setminus I} n_i$. Finally, it is straightforward to verify that, when $n_i \rightarrow n \quad \forall i \in T$, $\tilde{\alpha} \rightarrow \alpha$, and the complete interconnection graph K_n is again realized.

5. OTHER FORMS OF NEIGHBORING

Although [Algorithm 1](#) allows us to achieve maximum neighbor connectivity in the form of a complete graph resembling a GHZ state, it ultimately leads to a fixed outcome. The procedure is constrained to a particular set of gates on specific nodes and does not generalize

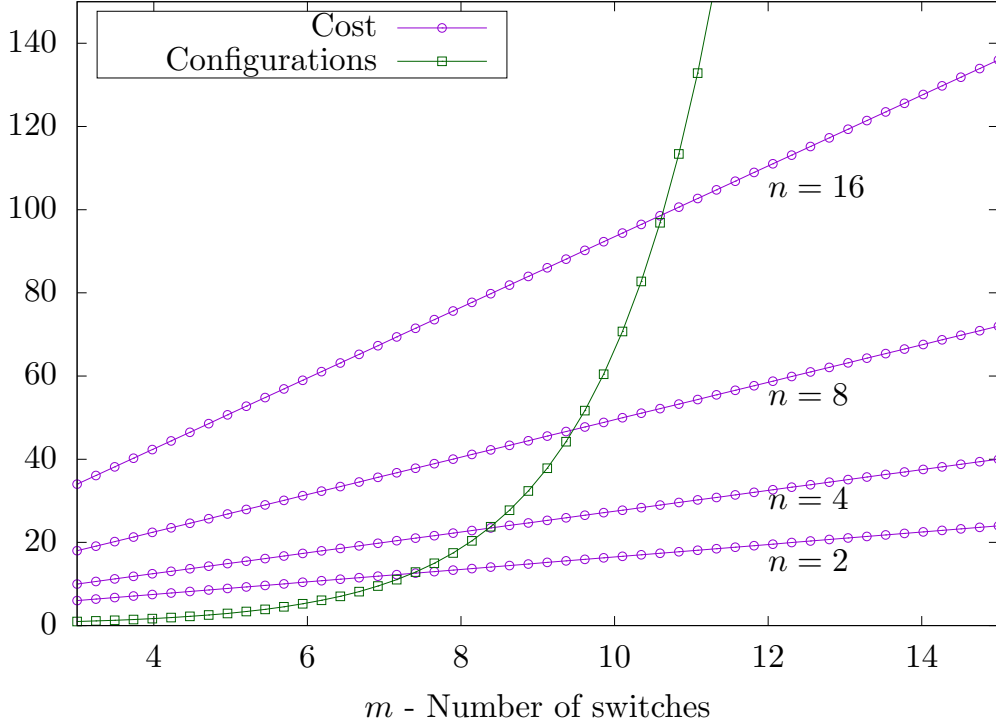


FIGURE 4. Cost of the graph state transformation vs. number of switches m and nodes per switch.

beyond these conditions. However, the results in [13] introduce a degree of flexibility in peer-to-peer connectivity, provided that a bi-star logical topology is first established. This Section is dedicated to achieving precisely that for our specific network configuration.

In order to obtain a bi-star configuration from an initial m -star configuration, we must perform a minimum of $\frac{m-1}{2}$ measurements—excluding the σ_Z measurements on the leaf nodes. This requirement becomes evident when considering the underlying structure of the algorithm. In the final step, we obtain a system consisting of two switches and their corresponding leaf nodes—one switch retaining the original leaves, while the other accumulates additional leaf nodes—connected via an intermediary switch without any leaf nodes. Applying a σ_X gate at this stage results in a star configuration that is locally equivalent to a complete graph. However, if instead a σ_Y is applied, the system transitions into a bi-star configuration.

While this particular case is not immediately compelling (since the resulting nodes maintain the same communication capabilities as in the original algorithm) selecting different switches for leaf node deletion allows for a broader range of communication possibilities. The challenge arises naturally from this intuition: we must identify $\frac{m-1}{2}$ nodes whose neighbors will be removed, followed by the application of the appropriate Pauli gates to establish a bi-star topology. The complexity of this task escalates rapidly, as it evolves into a combinatorial optimization problem: assuming an odd number m of switches, we would have $m-2$ switches from which to choose, and we must select $\frac{m-1}{2}$ of them. Hence, the number of possible configurations is $\binom{m-2}{\frac{m-1}{2}} \approx 2^{m/2}$

TABLE 1. Clients removed and corresponding transformations

Sw	First Step	Second Step	Result
$\{1, 3, 5\}$	Algorithm 1		Bi-star $(0, 6^\dagger)$
$\{1, 2, 3\}$	$\sigma_X(1, 0)$	$\sigma_X(3, 2)$	Tri-star $(4^\dagger, 5, 6)$
$\{2, 3, 4\}$	$\sigma_X(2, 1)$	$\sigma_X(4, 3)$	Tri-star $(0, 5^\dagger, 6)$
$\{1, 2, 4\}$	$\sigma_Y(1)$	$\sigma_X(4, 5), \sigma_X(2, 3)$	Bi-star $(0, 6^\dagger)$
$\{1, 2, 5\}$	$\sigma_Y(1)$	$\sigma_X(5, 4), \sigma_X(2, 3)$	Bi-star $(0^\dagger, 6^\dagger)$
$\{1, 3, 4\}$	$\sigma_Y(3)$	$\sigma_X(4, 5), \sigma_X(1, 2)$	Bi-star $(0, 6^\dagger)$

for large m , which becomes computationally unmanageable even for a relatively small number of switches (e.g., $m = 9$). The problem is more tractable if we exploit certain properties of the network topology. Since the network has an odd number of switches, it is always possible to identify a central switch located at position $\frac{m-1}{2}$. This central symmetry allows us to simplify the problem by treating several configurations as equivalent. Specifically, we can use the symmetry $i \rightarrow m - 1 - i$, $i = 0, \dots, \frac{m-1}{2}$, around this central node as identical configurations.

To illustrate this, we consider the example with $m = 7$ (the case $m = 5$ is trivial, as it results in only two distinct straightforward configurations). The number of distinct cases is $\binom{5}{3} = 10$, and the following symmetries hold $1 \leftrightarrow 5$, $2 \leftrightarrow 4$, 3 unchanged. Using these facts and exploring the few possibilities, we arrive at a total of 6 distinct cases, enumerated for the sake of illustration in Table 1. There are three distinct topological results, in terms of maximizing the number of neighboring connections, that arise when performing sequential gates on the network. The first result Sw_1, Sw_3, Sw_5 yields the same configuration as the one presented in Algorithm 1 and has already been studied. Another interesting configuration is the tri-star, a structure consisting of three star graphs joined at their central nodes – Tri-star $(4^\dagger, 5, 6)$ Tri-star $(0, 5^\dagger, 6)$. In this topology, one node, marked with \dagger , holds the majority of the clients, while the other two nodes retain their original connections. Although this sequence of gates does not maximize the number of neighboring connections, it enables different sets of allowed communications between nodes. A similar scenario occurs for Sw_1, Sw_2, Sw_4 arriving to the Bi-star $(0, 6^\dagger)$ topology. An intriguing case arises in the form Bi-star $(0^\dagger, 6^\dagger)$, where both switches hold a similar number of clients. If we were to follow standard protocols of removing all but one client from one of the nodes, we would compromise our goal of achieving maximum connectivity, thereby negating the intended purpose of this result. Instead, we adopt an alternative protocol in [13] to the realization of an extranet artificial topology, in our interpretation a bi-star topology interconnecting each client of one star with each client of the other. Precisely, through the sequence of gates $\sigma_X(0, 6) \rightarrow \sigma_Z(6)$, where nodes 6 and 0 are interchangeable, yielding the same configuration $|K_{n_1, n_2}\rangle$, where K_{n_1, n_2} denotes the complete bipartite graph with (n_1, n_2) in each class. Fig. 4 depicts the cost (number of measurements) of the proposed transformations.

6. DISCUSSION AND APPLICATION

6.1. Quantum Networks. Though the Quantum Internet has not yet been fully conceptualized, we adhere to the consensus that it would operate under similar principles as the classical Internet, supported by a suite of Quantum Internet protocols to enable seamless communication between devices. Thus, a Global Quantum Network will be composed of interconnected quantum sub-networks. Our proposal formalizes hierarchical networks composed of bi-star

and tri-star topologies, i.e., a Quantum Internet backbone plus Quantum Islands as a possible network-wide architecture.

This structure has already been demonstrated in QKD deployment (Euro QCI [19]), where each QKD domain has its own SDN controller responsible for intra-domain services, and these controllers communicate via an East-West Bound Interface to support inter-domain communication. Based upon this idea, we propose a hybrid model combining bipartite quantum networks and graph-state networks. In this model, intra-domain connectivity relies on bipartite entanglement distribution, ensuring better compatibility with classical communication and control, while graph states would enable the generation and manipulation of complex entangled states within each domain, aligning with the network topology. An architectural design featuring a two-layer network enables cluster reconfiguration, see [20]. Such techniques allow arbitrary networks to be transformed into structured configurations, such as multi-star networks, facilitating the efficient execution of the algorithms presented in this article.

6.2. Efficient Quantum Protocols. Graph states provide the necessary entanglement structure for secure and coordinated multi-party quantum protocols.

6.2.1. Multi-user QKD. One first application is multi-user QKD for an arbitrary subset S of users. Instead of constructing entanglement through bipartite links between all user pairs—requiring $\binom{|S|}{2}$ connections—a more efficient approach involves generating a GHZ state for all clients and discarding those not in S . While not optimal, this method eliminates the need for Steiner trees and significantly reduces resource overhead [21].

6.2.2. Quantum Conference Key Agreement (QCKA). This is a widely studied field that aims to extend Quantum Key Distribution (QKD) to multiple parties [22]. Consider a total of n users who wish to establish a shared secret key: Alice and the set of users Bob_1, \dots, Bob_{n-1} . This can be achieved using an n -partite GHZ state, which represents the final quantum state obtained in our protocols. A set of stabilizer measurements can be performed to detect potential eavesdroppers by establishing parity checks. Additionally, performing σ_Z or σ_X measurements on each node enables the full key to be extracted securely. Such configurations are essential for overcoming the limitations of bipartite entanglement, enabling multi-party Quantum Key Distribution (QKD) [23] and quantum secret sharing [8].

6.2.3. Distributed Quantum Computing. Another important application of graph states is found in grid topologies, where vertices are positioned at the intersections of a grid. This structure is particularly relevant for Distributed Quantum Computing (DQC) [24] and the widely used X protocol, which enables bipartite entanglement between any two nodes in the grid. This protocol is further optimized in [25], where improvements in resource efficiency and robustness against noise in dynamic and lossy networks are demonstrated.

7. CONCLUSIONS

In this work, we have extended and refined the methods proposed in [15] and [13], thereby enhancing their applicability and generality. Building upon these, we expanded their algorithm to a linear cluster architecture, where client nodes are attached to each of the central switches, arriving at a fixed maximum GHZ state for a multi-star network, depending on the number of switches m and their neighbors n . We worked out in full detail a particular network case for $m = 7$ switches and an arbitrary number of client nodes.

A key open problem is to derive a general result for node deletion, leveraging network symmetries and node selection strategies to mitigate the exponential growth in complexity. Further

exploration in this direction could lead to significant optimizations in large-scale quantum network architectures. A wider area for future research lies in the area of Distributed Quantum Computing (DQC); we point at exploring mesh and grid topologies to extract similar results to those of this paper.

REFERENCES

- [1] A. S. Cacciapuoti, M. Caleffi, F. Tafuri, F. S. Cataliotti, S. Gherardini, and G. Bianchi, “Quantum internet: Networking challenges in distributed quantum computing,” *IEEE Network*, vol. 34, no. 1, pp. 137–143, 2020.
- [2] Y. Shi, C. Liu, S. Stein, M. Wang, M. Zheng, and A. Li, “Design of an entanglement purification protocol selection module,” 2024.
- [3] R. Valivarthi and e. a. Davis, “Teleportation systems toward a quantum internet,” *PRX Quantum*, vol. 1, p. 020317, Dec 2020.
- [4] J. Walln fer, A. Pirker, M. Zwerger, and W. D r, “Multipartite state generation in quantum networks with optimal scaling,” *Scientific Reports*, vol. 9, no. 1, Jan. 2019.
- [5] M. Hein, W. D r, J. Eisert, R. Raussendorf, M. V. den Nest, and H. J. Briegel, “Entanglement in graph states and its applications,” 2006.
- [6] M. Van den Nest, J. Dehaene, and B. De Moor, “Graphical description of the action of local clifford transformations on graph states,” *Physical Review A*, vol. 69, no. 2, Feb. 2004.
- [7] O. G hne, G. T th, P. Hyllus, and H. J. Briegel, “Bell inequalities for graph states,” *Phys. Rev. Lett.*, vol. 95, p. 120405, Sep 2005.
- [8] D. Markham and B. C. Sanders, “Graph states for quantum secret sharing,” *Phys. Rev. A*, vol. 78, p. 042309, Oct 2008.
- [9] L. Vandr , J. de Jong, F. Hahn, A. Burchardt, O. G hne, and A. Pappa, “Distinguishing graph states by the properties of their marginals,” 2024.
- [10] B. A. Bell *et al.*, “Experimental demonstration of graph-state quantum secret sharing,” *Nature Communications*, vol. 5, no. 1, p. 5480, Nov 2014.
- [11] J. Huang *et al.*, “Chip-based photonic graph states,” *AAPPS Bulletin*, vol. 33, no. 1, p. 14, Jun 2023.
- [12] N. Benchasattabuse, M. Hajdu ek, and R. V. Meter, “Architecture and protocols for all-photonic quantum repeaters,” 2024.
- [13] S.-Y. Chen, J. Illiano, A. S. Cacciapuoti, and M. Caleffi, “Entanglement-based artificial topology: Neighboring remote network nodes,” 2024.
- [14] F. Mazza, M. Caleffi, and A. S. Cacciapuoti, “Intra-qian connectivity: beyond the physical topology,” 06 2024.
- [15] J. de Jong, F. Hahn, N. Tcholtchev, M. Hauswirth, and A. Pappa, “Extracting ghz states from linear cluster states,” *Phys. Rev. Res.*, vol. 6, p. 013330, Mar 2024.
- [16] H. Aschauer, W. D r, and H.-J. Briegel, “Multiparticle entanglement purification for two-colorable graph states,” *Phys. Rev. A*, vol. 71, p. 012319, Jan 2005.
- [17] M. Hein, J. Eisert, and H. J. Briegel, “Multiparty entanglement in graph states,” *Phys. Rev. A*, vol. 69, p. 062311, Jun 2004.
- [18] F. Mazza, M. Caleffi, and A. S. Cacciapuoti, “Quantum lan: On-demand network topology via two-colorable graph states,” in *2024 International Conference on Quantum Communications, Networking, and Computing (QNCN)*, 2024, pp. 127–134.
- [19] M. I. Garcia-Cid, L. Ortiz, J. Saez, and V. Martin, “Strategies for the integration of quantum networks for a future quantum internet,” 2024.
- [20] C. Clayton, X. Wu, and B. Bhattacharjee, “Efficient routing on quantum networks using adaptive clustering,” 2024.
- [21] S. S. Chelluri, S. Khatri, and P. van Loock, “Multipartite entanglement distribution in bell-pair networks without steiner trees and with reduced gate cost,” 2025.
- [22] G. Murta, F. Grasselli, H. Kampermann, and D. Bru , “Quantum conference key agreement: A review,” *Advanced Quantum Technologies*, vol. 3, no. 11, Sep. 2020.
- [23] Y. Qian, Z. Shen, G. He, and G. Zeng, “Quantum-cryptography network via continuous-variable graph states,” *Phys. Rev. A*, vol. 86, p. 052333, Nov 2012.
- [24] Y. Mao, Y. Liu, X. Shang, and Y. Yang, “Network topology design for distributed quantum computing,” in *2024 IEEE 44th International Conference on Distributed Computing Systems (ICDCS)*, 2024, pp. 1213–1223.

[25] R. Negrin, N. Dirneger, W. Munizzi, J. Talukdar, and P. Narang, “Efficient multiparty entanglement distribution with dodag-x protocol,” 2024.

Since the graph is bicolorable (coloring scheme shown in Fig. 2), we define two subsets of nodes and the edge set as $E = E_S \cup E_{n_i}$ where E_S represents the sequential connections between switches, while E_{n_i} represents the connections between each switch and its leaf nodes K_j^i . Thus, the graph is given by $G = (P_0, P_1, E)$.

$$\begin{aligned} P_0 &= \{Sw_{2i}\}_{i=0}^{\frac{m-1}{2}} \cup \{K_j^{2i+1}\}_{j=1, i=0}^{n, \frac{m-3}{2}}, \\ P_1 &= \{Sw_{2i+1}\}_{i=0}^{\frac{m-3}{2}} \cup \{K_j^{2i}\}_{j=1, i=0}^{n, \frac{m-1}{2}}, \\ E_S &= \{(Sw_i, Sw_{i+1})\}_{i=0}^{m-2}, \quad E_{n_i} = \{(Sw_i, K_j^i)\}_{j=1, i=0}^{n, m-1}. \end{aligned}$$

Following Algorithm 1, we start by selecting alternating nodes, beginning with Sw_0 (they align with the odd-labeled switches). Then, apply σ_Z measurements on their leaf nodes, modifying P_0 while leaving P_1 unchanged. As a result, the edge set is updated to

$$\begin{aligned} P'_0 &= \{Sw_{2i}\}_{i=0}^{\frac{m-1}{2}}, \quad P'_1 = P_1. \\ E'_S &= E_S, \quad E'_{n_i} = \{(Sw_{2i}, K_j^{2i})\}_{j=1, i=0}^{n, \frac{m-1}{2}}, \end{aligned}$$

where $E' = E_S \cup E'_{n_i}$. The modified graph is therefore $G' = (P'_0, P_1, E')$. Next, we perform a σ_X operation on every odd switch, where the σ_X operator acts as $\sigma_X(G)_{\alpha, \beta} = \tau_\beta(\tau_\alpha(\tau_\beta(G)) - \alpha)$. To illustrate this process, consider a minimal cell affected by a σ_X operation when applied at $\alpha = Sw_{2i+1}$ with $\beta = Sw_{2i}$. The relevant node subset is

$$\begin{aligned} \tilde{V} &= \{Sw_{2i+1}, Sw_{2i}, Sw_{2i-1}, Sw_{2i+2}, K_j^{2i}, K_j^{2i+2}\}_{j=1}^n \\ \tilde{E} &= \{(Sw_l, Sw_{l+1})\}_{l=2i-1}^{2i+1} \cup \{(Sw_h, K_j^h)\}_{j=1}^n \end{aligned}$$

where $h = \{2i, 2i+2\}$. Local complementation at vertex Sw_{2i} results in a complete graph on the subset $V = \{Sw_{2i-1}, Sw_{2i+1}, Sw_{2i}, K_j^{2i}\}_{j=1}^n$. Since no neighboring nodes of Sw_{2i} were previously connected, new edges appear

$$\begin{aligned} \tilde{E}' &= \{(K_j^{2i}, K_h^{2i})\}_{j \neq h} \cup \{(Sw_{2i-1}, Sw_{2i+1})\} \cup \\ &\quad \{(Sw_{2i-1}, K_j^{2i})\}_{j=1}^n \cup \{(Sw_{2i+1}, K_j^{2i})\}_{j=1}^n. \end{aligned}$$

Additionally, Sw_{2i+2} becomes connected to Sw_{2i+1} along with its leaf nodes K_j^{2i+2} . Performing local complementation at Sw_{2i+1} removes the edges within the previously complete subgraph, yielding the updated edge set

$$\begin{aligned} \tilde{E}'' &= (Sw_{2i+1}, \{Sw_{2i}, Sw_{2i-1}, Sw_{2i+2}, K_j^{2i}\}_{j=1}^n) \cup \\ &\quad (Sw_{2i+2}, \{Sw_{2i}, Sw_{2i-1}, K_j^{2i}, K_j^{2i+2}\}_{j=1}^n). \end{aligned}$$

Since the next step is the deletion of Sw_{2i+1} , all its connections are removed, leading to the new graph $\tilde{V}''' = \{Sw_{2i-1}, Sw_{2i}, Sw_{2i+2}, K_j^{2i}, K_j^{2i+2}\}_{j=1}^n$, $\tilde{E}''' = Sw_{2i+2} \times \{Sw_{2i}, Sw_{2i-1}, K_j^{2i}, K_j^{2i+2}\}_{j=1}^n$. This structure corresponds to a star graph centered at Sw_{2i+2} . Finally, since Sw_{2i} has only one neighbor, the local complementation operation at Sw_{2i} is trivial, leaving the graph unchanged. By iterating this process throughout the network, we find that the final output of the algorithm is a larger star graph consisting of all even-indexed switches and their respective leaf nodes Sw_{2i}, K_j^{2i} , $\forall i \in \{0, \frac{m-1}{2}\}$, $j \in \{1, n\}$. This graph is locally equivalent to a complete

graph of the same size, which can be achieved by performing a local complementation at its central vertex. \square

Email address: mveiga@det.uvigo.es avilas@uvigo.es rebeca@det.uvigo.es

ATLANTTIC, UNIVERSIDADE DE VIGO, SPAIN